Nuclei Segmentation in Histopathology Images

Deniz Mercadier Sayın*, Beril Besbinar†, Pascal Frossard†

May 16, 2019

†EPFL - Signal Processing Laboratory (LTS4)

Motivation

Why histopathology images?

- Common practice of digital pathology

Motivation

Why histopathology images?

- Common practice of digital pathology
  Hematoxylin and Eosin (H&E) stain is one of the principal stains

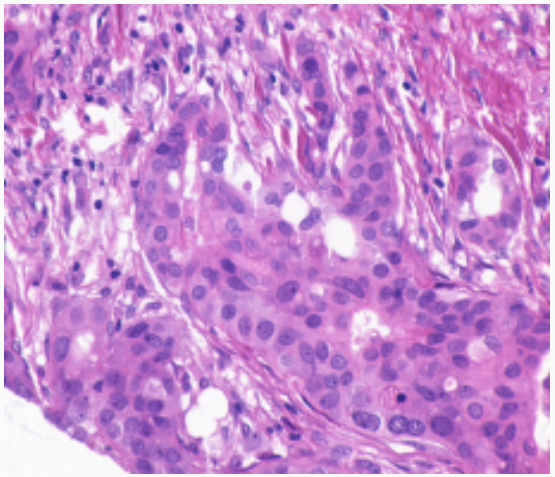

Motivation

Why histopathology images?

- Common practice of digital pathology

Why nuclei segmentation?

- Cancer diagnosis, grading and prognosis
- Valuable information such as size, texture and shape

Motivation

Why histopathology images?

- Common practice of digital pathology

Why nuclei segmentation?

- Cancer diagnosis, grading and prognosis
- Valuable information such as size, texture and shape

What are the challenges?

- Variation of nuclear size and shape
- Variations in staining techniques

Motivation

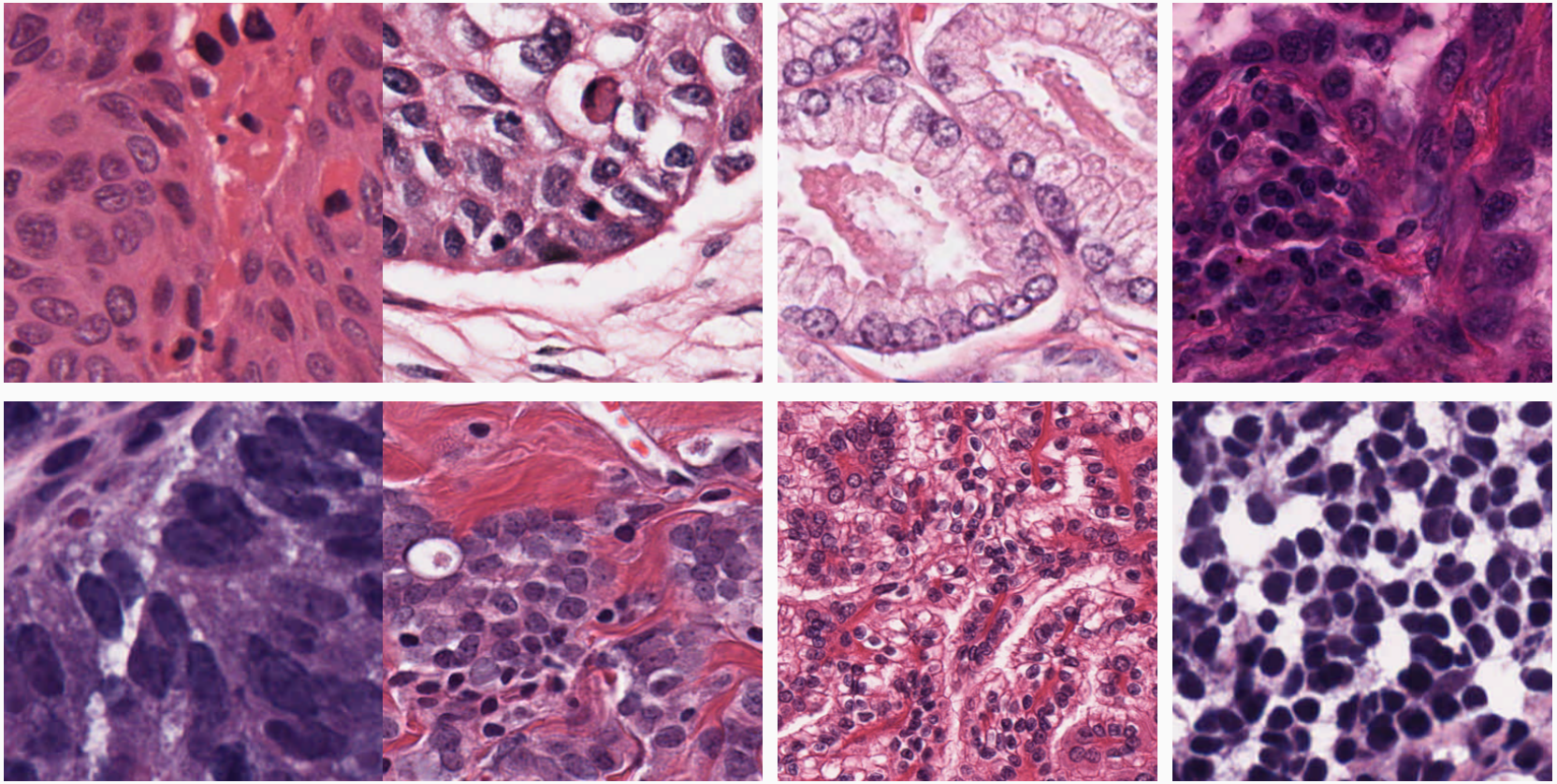

Existing Methods

Traditional approaches

- (Optional) Pre-processing/color normalization
- Feature extraction (color, texture, shape-based)
- Pixel-wise classifier or watershed/graph-cut
- (Optional) Post-processing for cluttered nuclei

Existing Methods

Traditional approaches

- (Optional) Pre-processing/color normalization
- Feature extraction (color, texture, shape-based)
- Pixel-wise classifier or watershed/graph-cut
- (Optional) Post-processing for cluttered nuclei

Deep Learning (DL) approaches

- (Optional) Pre-processing/color normalization
- Pixel-wise classification using the patches around pixels
  Merging two tasks have already improved the performance
- (Optional) Post-processing for cluttered nuclei

Existing Methods - DL approaches

Classification at each pixel

Existing Methods - DL approaches

Classification at each pixel $\leftarrow$ Final mask is obtained via a sliding window

Existing Methods - DL approaches

Classification at each pixel $\leftarrow$ Final mask is obtained via a sliding window

Redundant computation of features and increased computational expense

Existing Methods - DL approaches

Classification at each pixel ← Final mask is obtained via a sliding window

Redundant computation of features and increased computational expense

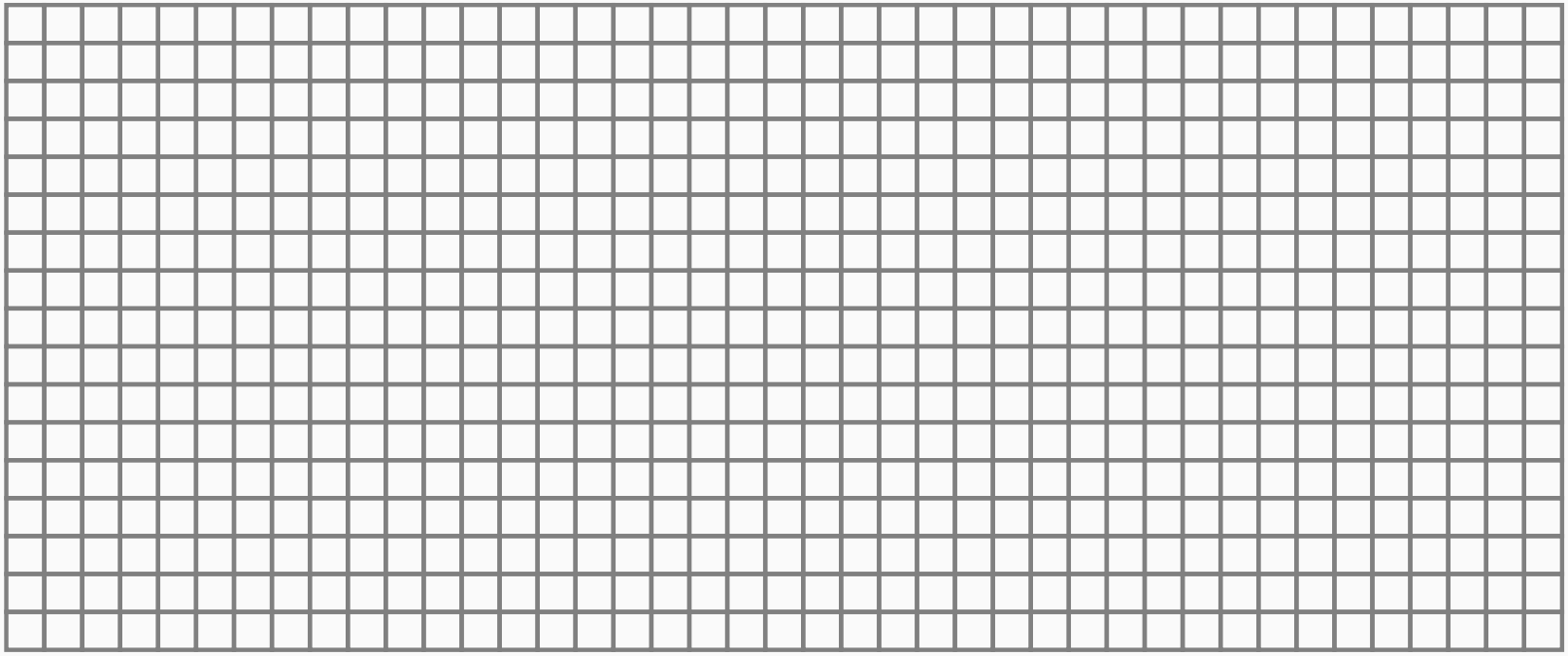

Existing Methods - DL approaches

Classification at each pixel ← Final mask is obtained via a sliding window

Redundant computation of features and increased computational expense

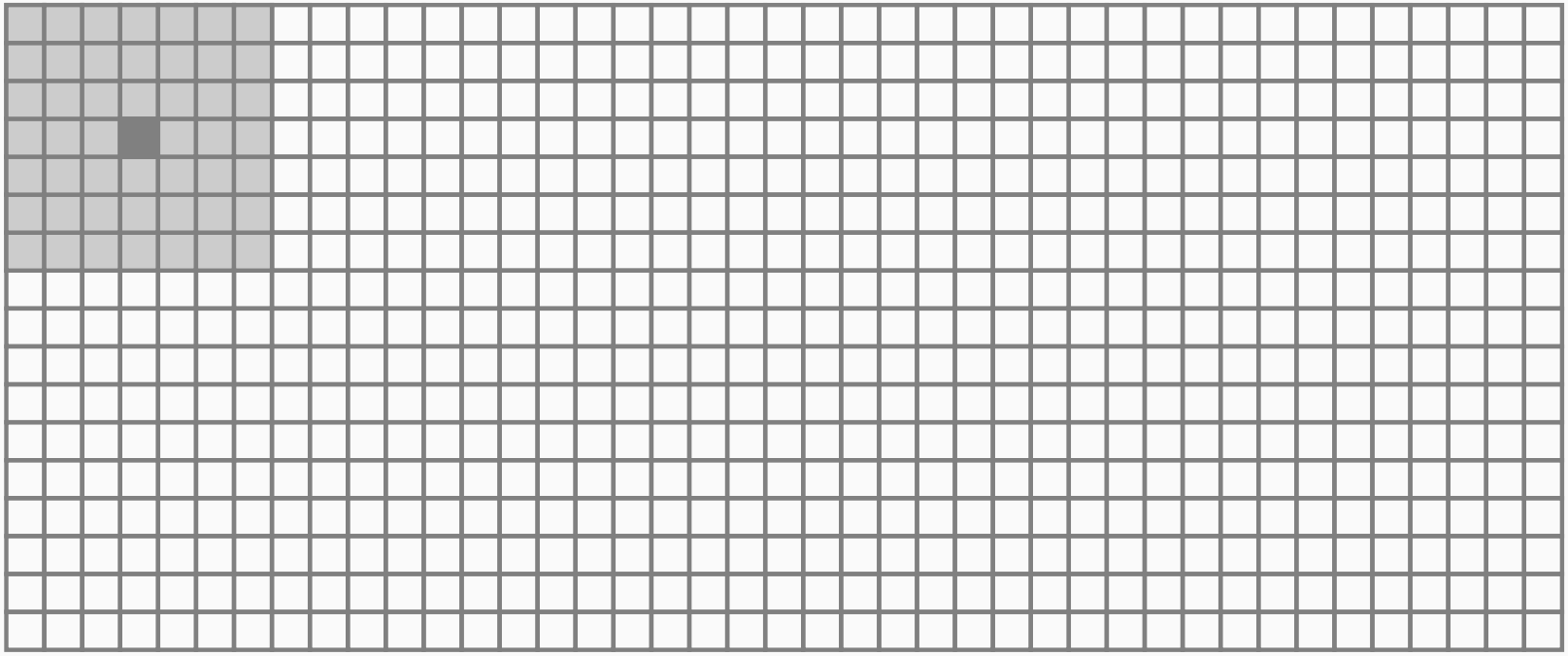

Existing Methods - DL approaches

Classification at each pixel ← Final mask is obtained via a sliding window

Redundant computation of features and increased computational expense

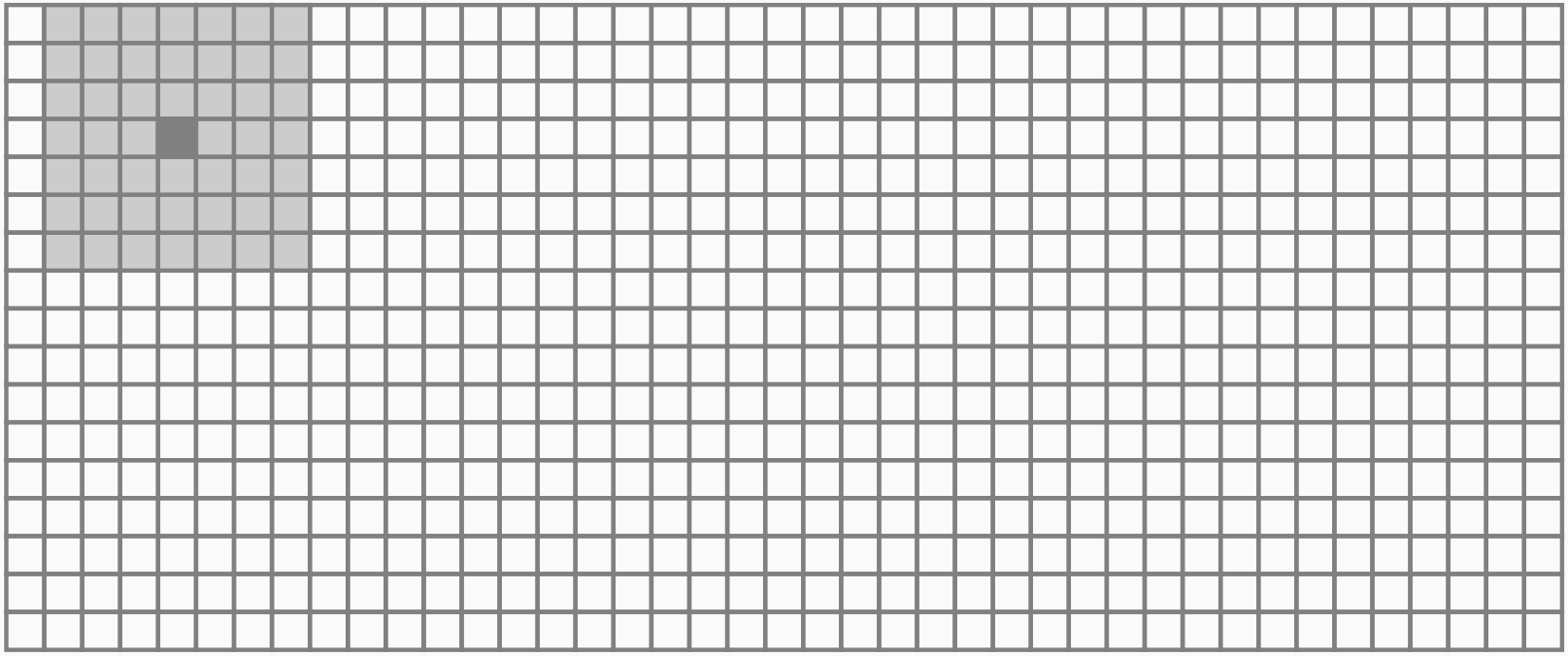

Existing Methods - DL approaches

Classification at each pixel ← Final mask is obtained via a sliding window

Redundant computation of features and increased computational expense

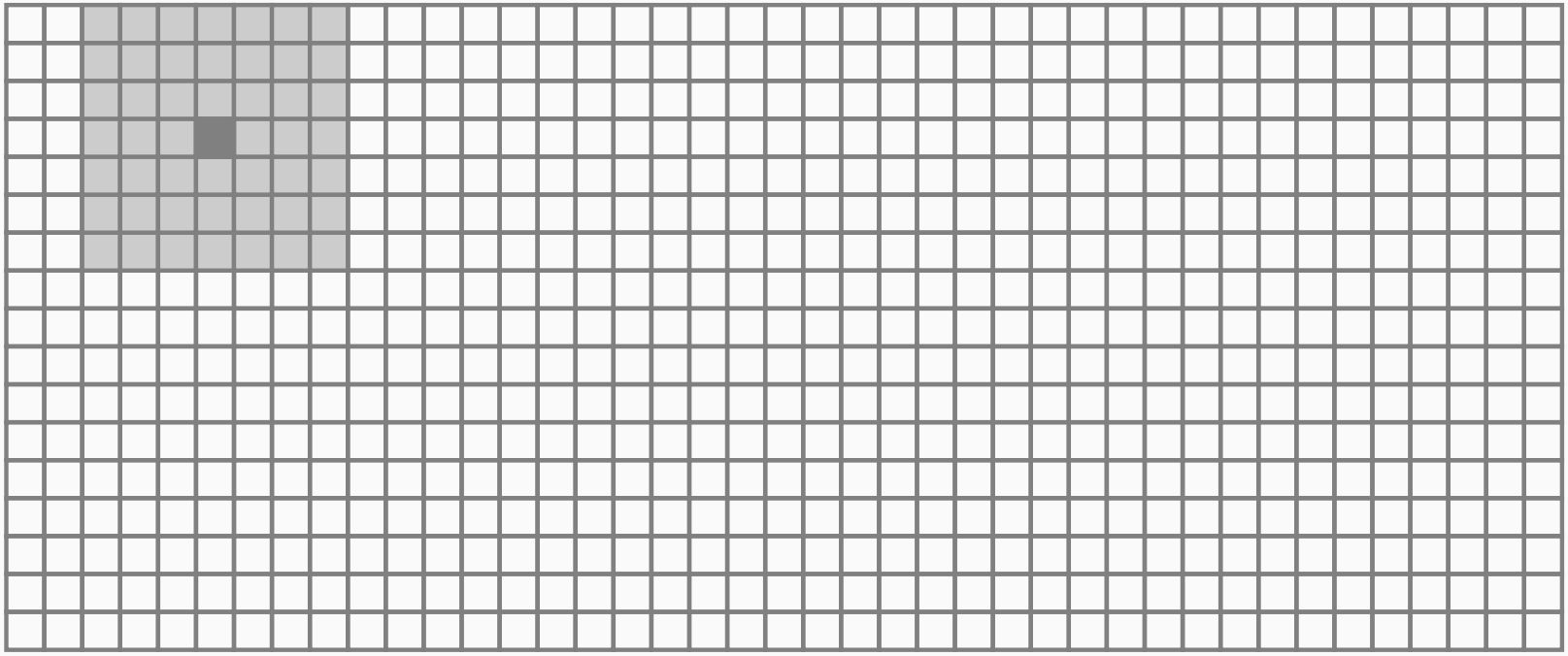

Existing Methods - DL approaches

Existing Methods - DL approaches

1. Janowczyk et al. : binary classification of pixels using patches of size 32x32

[1] Janowczyk, A., and Madabhushi, A., “Deep learning for digital pathology image analysis: A comprehensive tutorial with selected use cases,” Journal of pathology informatics, 2016.

Existing Methods - DL approaches

1 Janowczyk et al. : binary classification of pixels using patches of size 32x32

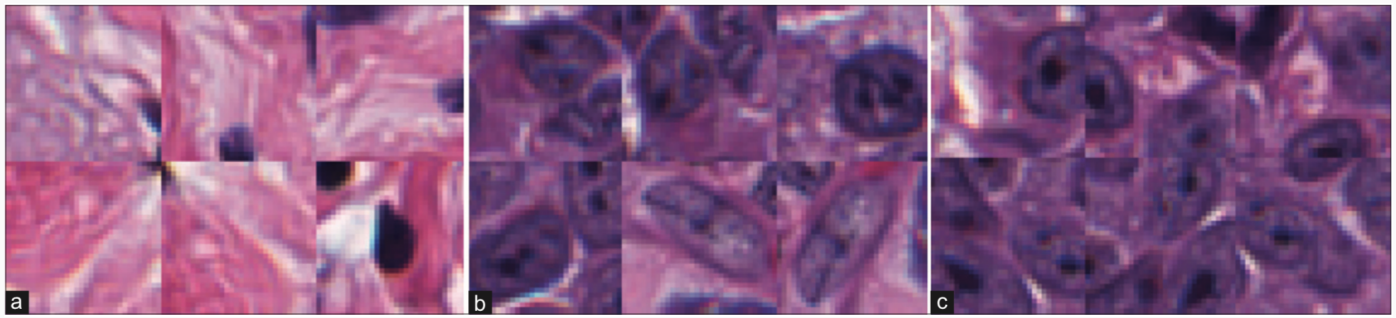

Existing Methods - DL approaches

1. Janowczyk et al. : binary classification of pixels using patches of size 32x32
2. Kumar et al. : 3-way classification - nuclei, nuclei boundary, background

[1] Janowczyk, A., and Madabhushi, A., “Deep learning for digital pathology image analysis: A comprehensive tutorial with selected use cases,” Journal of pathology informatics, 2016.
[2] Kumar, N., Verma, R., Sharma, S., Bhargava, S., Vahadane, A., and Sethi, A.,“A dataset and a technique for generalized nuclear segmentation for computational pathology,”IEEE transactions on medical imaging, 2017.

Existing Methods - DL approaches

1. Janowczyk et al. : binary classification of pixels using patches of size 32x32
2. Kumar et al. : 3-way classification - nuclei, nuclei boundary, background

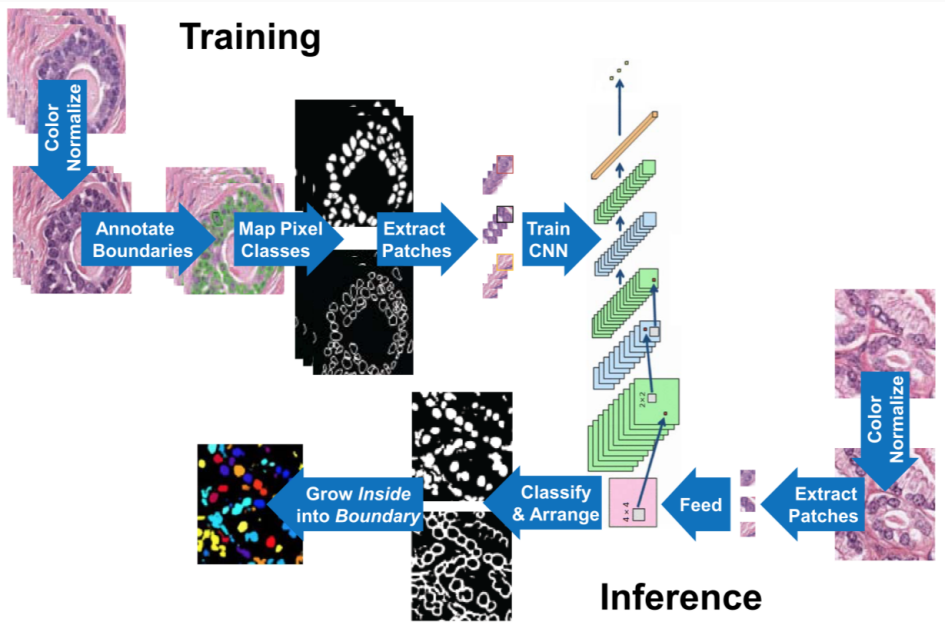

Existing Methods - DL approaches

1. Janowczyk et al. : binary classification of pixels using patches of size 32x32
2. Kumar et al. : 3-way classification - nuclei, nuclei boundary, background
3. Naylor et al. : Regression to the distance map

[1] Janowczyk, A., and Madabhushi, A., “Deep learning for digital pathology image analysis: A comprehensive tutorial with selected use cases,” Journal of pathology informatics, 2016.
[2] Kumar, N., Verma, R., Sharma, S., Bhargava, S., Vahadane, A., and Sethi, A.,“A dataset and a technique for generalized nuclear segmentation for computational pathology,”IEEE transactions on medical imaging, 2017.
[3] Naylor, P., La´e ,M., Reyal, F., and Walter, T., “Segmentation of nuclei in histopathology images by deep regression of the distance map,”IEEE Transactions on Medical Imaging, 2018

Existing Methods - DL approaches

1. Janowczyk et al. : binary classification of pixels using patches of size 32x32
2. Kumar et al. : 3-way classification - nuclei, nuclei boundary, background
3. Naylor et al. : Regression to the distance map

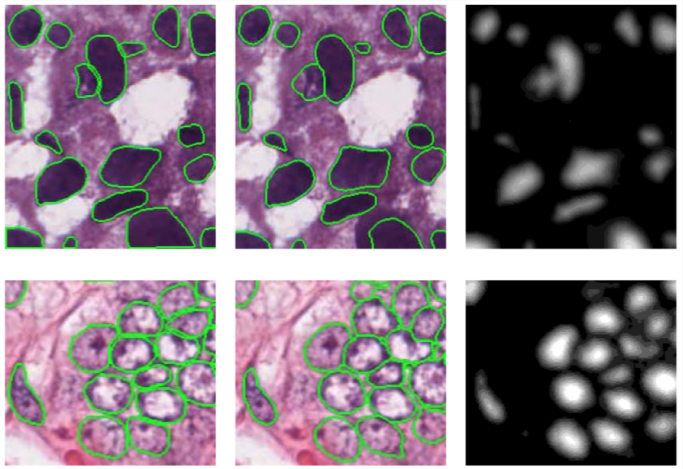

Method

Formulation of the problem as segmentation in a holistic manner rather than classification of patches:

Method

Formulation of the problem as segmentation in a holistic manner rather than classification of patches:

- Dataset: Partially annotated dataset introduced in *Janowczyk et al.*

Method

Formulation of the problem as segmentation in a holistic manner rather than classification of patches:

- Dataset: Partially annotated dataset introduced in *Janowczyk et al.*
- Adaptation of loss function to partially annotated dataset

Method

Formulation of the problem as segmentation in a holistic manner rather than classification of patches:

- Dataset: Partially annotated dataset introduced in *Janowczyk et al.*
- Adaptation of loss function to partially annotated dataset
- Architecture: U-Net (with modifications)

Method - Dataset

The dataset introduced in [1]:

141 Hematoxylin and Eosin (H&E) stained images

[1] Janowczyk, A., and Madabhushi, A., “Deep learning for digital pathology image analysis: A comprehensive tutorial with selected use cases,” Journal of pathology informatics, 2016.

Method - Dataset

The dataset introduced in [1]:

141 Hematoxylin and Eosin (H&E) stained images

- of size 2000 x 2000
- at 40x magnification
- with partial annotations.

[1] Janowczyk, A., and Madabhushi, A., “Deep learning for digital pathology image analysis: A comprehensive tutorial with selected use cases,” Journal of pathology informatics, 2016.

Method - Dataset

The dataset introduced in [1]:

141 Hematoxylin and Eosin (H&E) stained images

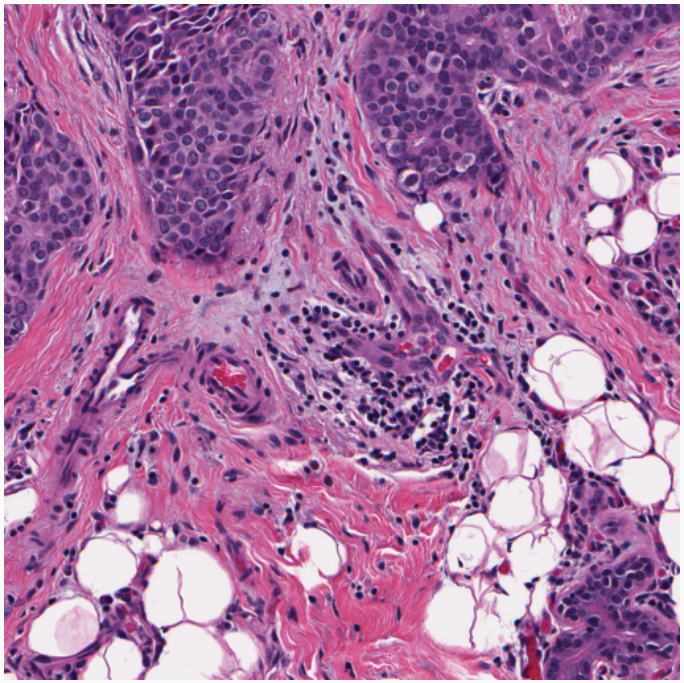

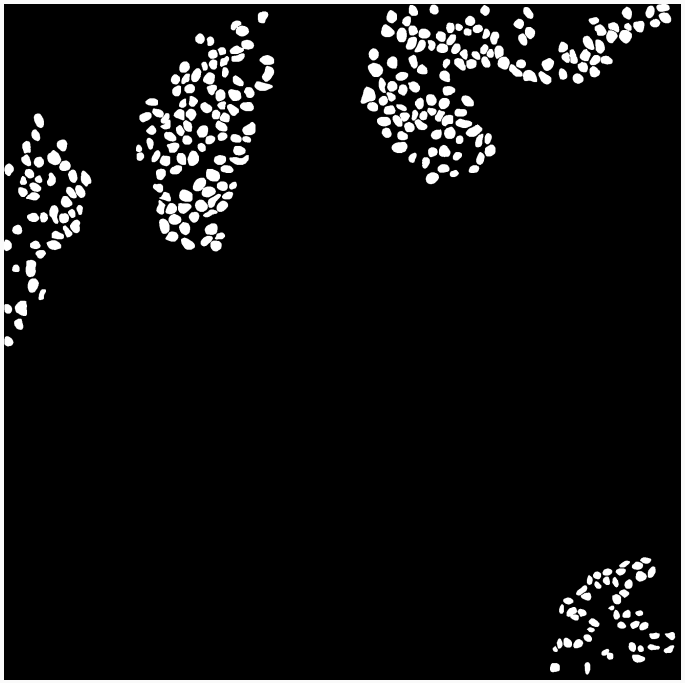

[1] Janowczyk, A., and Madabhushi, A., “Deep learning for digital pathology image analysis: A comprehensive tutorial with selected use cases,” Journal of pathology informatics, 2016.

Method - Dataset

The dataset introduced in [1]:

141 Hematoxylin and Eosin (H&E) stained images

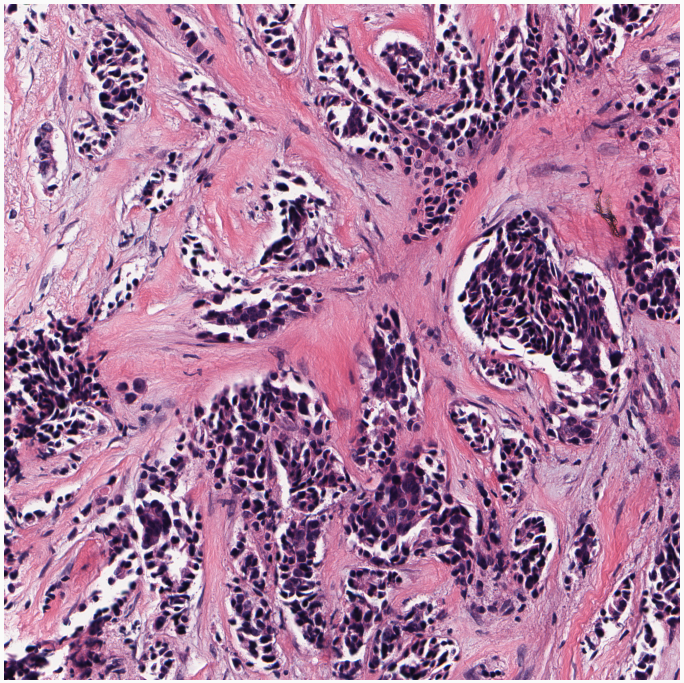

[1] Janowczyk, A., and Madabhushi, A., “Deep learning for digital pathology image analysis: A comprehensive tutorial with selected use cases,” Journal of pathology informatics, 2016.

Method - Loss

labels: $y_{ij} \in \{0, 1\}$ $\begin{cases} y_{ij} = 1 : \text{nuclei} \\ y_{ij} = 0 : \text{non-nuclei/not-annotated} \end{cases}$

predicted labels: $\hat{y}_{ij}^{\text{fg}}, \hat{y}_{ij}^{\text{bg}} \in [0, 1], \quad \hat{y}_{ij} = \begin{cases} 1 & \text{if} \quad \hat{y}_{ij}^{\text{fg}} \geq \hat{y}_{ij}^{\text{bg}} \\ 0 & \text{if} \quad \hat{y}_{ij}^{\text{fg}} < \hat{y}_{ij}^{\text{bg}} \end{cases}$

Method - Loss

labels: $y_{ij} \in \{0, 1\}$ $\begin{cases} y_{ij} = 1 : \text{nuclei} \\ y_{ij} = 0 : \text{non-nuclei/not-annotated} \end{cases}$

predicted labels: $\hat{y}_{ij}^{\text{fg}}, \hat{y}_{ij}^{\text{bg}} \in [0, 1], \quad \hat{y}_{ij} = \begin{cases} 1 & \text{if} \quad \hat{y}_{ij}^{\text{fg}} \geq \hat{y}_{ij}^{\text{bg}} \\ 0 & \text{if} \quad \hat{y}_{ij}^{\text{fg}} < \hat{y}_{ij}^{\text{bg}} \end{cases}$

$$\mathcal{L} = \sum_{(i,j) \in WxH} y_{ij} \log \hat{y}_{ij}^{\text{fg}} + (1 - y_{ij}) \log \hat{y}_{ij}^{\text{bg}}$$

Method - Loss

labels: $y_{ij} \in \{0, 1\}$ $\begin{cases} y_{ij} = 1 : \text{nuclei} \\ y_{ij} = 0 : \text{non-nuclei/not-annotated} \end{cases}$

predicted labels: $\hat{y}_{ij}^{\text{fg}}, \hat{y}_{ij}^{\text{bg}} \in [0, 1], \quad \hat{y}_{ij} = \begin{cases} 1 & \text{if} \quad \hat{y}_{ij}^{\text{fg}} \geq \hat{y}_{ij}^{\text{bg}} \\ 0 & \text{if} \quad \hat{y}_{ij}^{\text{fg}} < \hat{y}_{ij}^{\text{bg}} \end{cases}$

$$\mathcal{L} = \sum_{(i,j) \in WxH} y_{ij} \log \hat{y}_{ij}^{\text{fg}} + m_{ij} (1 - y_{ij}) \log \hat{y}_{ij}^{\text{bg}}$$

Method - Loss

labels: $y_{ij} \in \{0, 1\}$ $\begin{cases} y_{ij} = 1 : \text{nuclei} \\ y_{ij} = 0 : \text{non-nuclei/not-annotated} \end{cases}$

predicted labels: $\hat{y}_{ij}^{\text{fg}}, \hat{y}_{ij}^{\text{bg}} \in [0, 1], \quad \hat{y}_{ij} = \begin{cases} 1 & \text{if} \quad \hat{y}_{ij}^{\text{fg}} \geq \hat{y}_{ij}^{\text{bg}} \\ 0 & \text{if} \quad \hat{y}_{ij}^{\text{fg}} < \hat{y}_{ij}^{\text{bg}} \end{cases}$

$$\mathcal{L} = \sum_{(i,j) \in WxH} y_{ij} \log \hat{y}_{ij}^{\text{fg}} + m_{ij} (1 - y_{ij}) \log \hat{y}_{ij}^{\text{bg}}$$

$$d_{ij} = \min_{\substack{(i,j),(u,v) \in WxH \\ \{(i,j) \mid y_{ij}=1\}}} (\sqrt{(i-u)^2 + (j-v)^2})$$

$$m_{ij} = \begin{cases} 1, & \text{if} \quad d_{ij} \leq \alpha \\ e^{-\beta(d_{ij} - \alpha)}, & \text{if} \quad d_{ij} > \alpha \end{cases}$$

Method - Loss

labels: $y_{ij} \in \{0, 1\}$ $\begin{cases} y_{ij} = 1 : \text{nuclei} \\ y_{ij} = 0 : \text{non-nuclei/not-annotated} \end{cases}$

predicted labels: $\hat{y}_{ij}^{\text{fg}}, \hat{y}_{ij}^{\text{bg}} \in [0, 1], \quad \hat{y}_{ij} = \begin{cases} 1 & \text{if} \quad \hat{y}_{ij}^{\text{fg}} \geq \hat{y}_{ij}^{\text{bg}} \\ 0 & \text{if} \quad \hat{y}_{ij}^{\text{fg}} < \hat{y}_{ij}^{\text{bg}} \end{cases}$

$$\mathcal{L} = \sum_{(i,j) \in WxH} y_{ij} \log \hat{y}_{ij}^{\text{fg}} + \hat{m}_{ij} (1 - y_{ij}) \log \hat{y}_{ij}^{\text{bg}}$$

$$d_{ij} = \min_{\substack{(i,j),(u,v) \in WxH \\ \{(i,j) \mid y_{ij}=1\}}} (\sqrt{(i-u)^2 + (j-v)^2})$$

$$m_{ij} = \begin{cases} 1, & \text{if} \quad d_{ij} \leq \alpha \\ e^{-\beta(d_{ij} - \alpha)}, & \text{if} \quad d_{ij} > \alpha \end{cases}$$

$$\hat{m}_{ij} = m_{ij} \uplus \lambda(\mathbf{b} \ominus c)$$

Method - Loss

labels: $y_{ij} \in \{0, 1\}$ $\begin{cases} y_{ij} = 1 : \text{nuclei} \\ y_{ij} = 0 : \text{non-nuclei/not-annotated} \end{cases}$

predicted labels: $\hat{y}_{ij}^{\text{fg}}, \hat{y}_{ij}^{\text{bg}} \in [0, 1], \quad \hat{y}_{ij} = \begin{cases} 1 & \text{if} \quad \hat{y}_{ij}^{\text{fg}} \geq \hat{y}_{ij}^{\text{bg}} \\ 0 & \text{if} \quad \hat{y}_{ij}^{\text{fg}} < \hat{y}_{ij}^{\text{bg}} \end{cases}$

$$\mathcal{L} = \sum_{(i,j) \in WxH} y_{ij} \log \hat{y}_{ij}^{\text{fg}} + \hat{m}_{ij}(1 - y_{ij}) \log \hat{y}_{ij}^{\text{bg}} + \underbrace{\gamma \| w \|_2^2}_{w\text{:parameters}}$$

$$d_{ij} = \min_{\substack{(i,j),(u,v) \in WxH \\ \{(i,j) \mid y_{ij}=1\}}} (\sqrt{(i-u)^2 + (j-v)^2})$$

$$m_{ij} = \begin{cases} 1, & \text{if} \quad d_{ij} \leq \alpha \\ e^{-\beta(d_{ij} - \alpha)}, & \text{if} \quad d_{ij} > \alpha \end{cases}$$

$$\hat{m}_{ij} = m_{ij} \uplus \lambda(\mathbf{b} \ominus c)$$

Method - Background Modelling

$$\hat{m}_{ij} = m_{ij} \uplus \lambda(\mathbf{b} \ominus c)$$

Method - Background Modelling

$$\hat{m}_{ij} = m_{ij} \uplus \lambda(\mathbf{b} \ominus c)$$

$\mathbf{b}$ is obtained via unsupervised clustering

Method - Background Modelling

$$\hat{m}_{ij} = m_{ij} \uplus \lambda(\mathbf{b} \ominus c)$$

$\mathbf{b}$ is obtained via unsupervised clustering

k-means (k=2) using H,E,D channels:

OD_R	OD_G	OD_B	
0.18	0.20	0.08	Hematoxylin
0.01	0.13	0.01	Eosin
0.10	0.21	0.29	DAB

[4] Ruifrok, A. C., and Johnston, D. A., "Quantification of histochemical staining by color deconvolution" Analytical and quantitative cytology and histology the International Academy of Cytology [and] American Society of Cytology, 2001.

Method - Background Modelling

$$\hat{m}_{ij} = m_{ij} \uplus \lambda(\mathbf{b} \ominus c)$$

$\mathbf{b}$ is obtained via unsupervised clustering

k-means (k=2) using H,E,D channels:

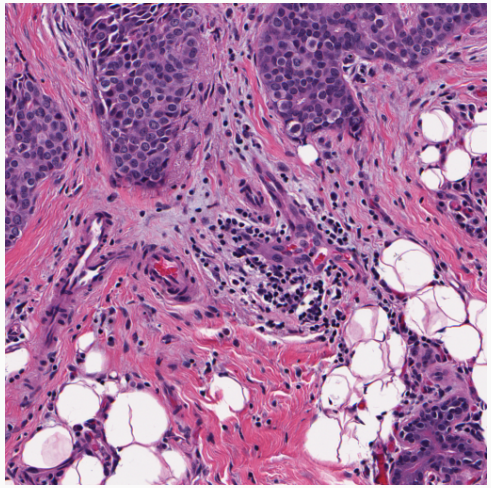
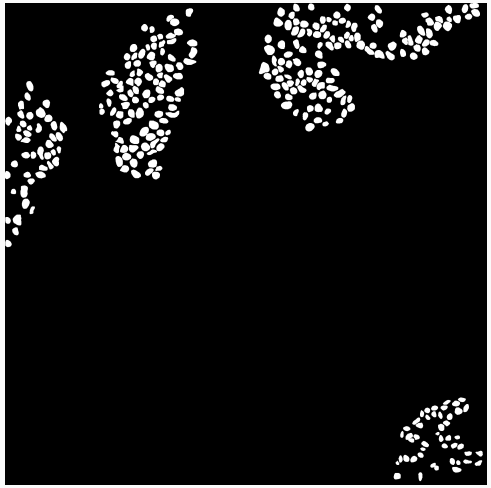
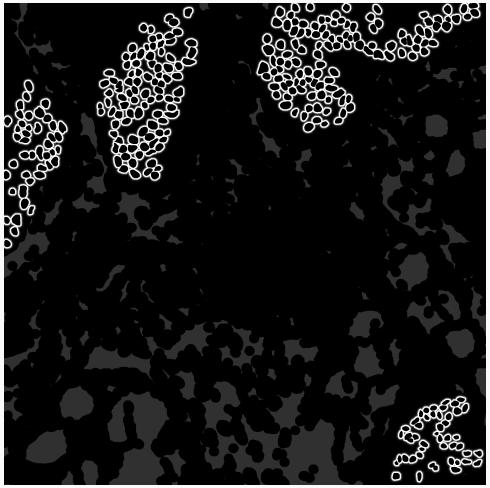

Method - Background Modelling

$$\hat{m}_{ij} = m_{ij} \uplus \lambda(\mathbf{b} \ominus c)$$

$\mathbf{b}$ is obtained via unsupervised clustering

k-means (k=2) using H,E,D channels:

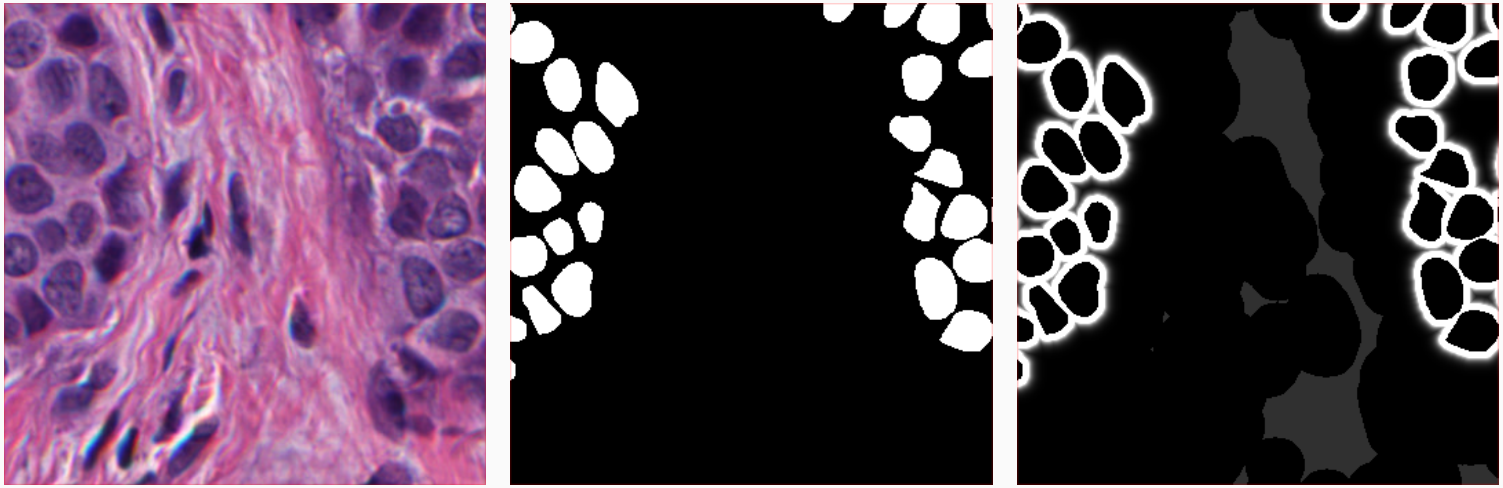

Method - Architecture

U-Net with 4 convolutional-deconvolutional layers

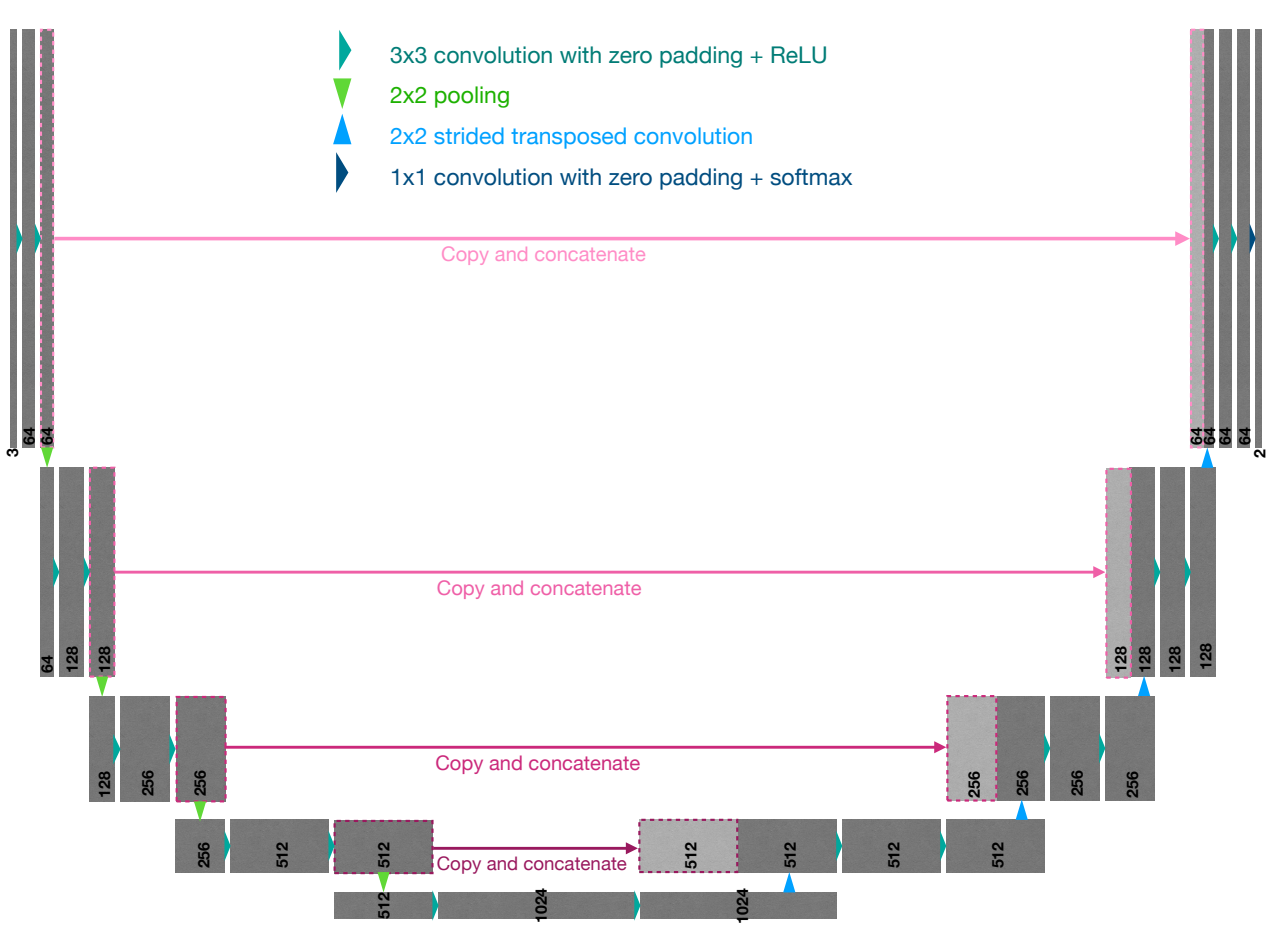

Method - Architecture

U-Net with 4 convolutional-deconvolutional layers

Architecture search:

- Different numbers of convolutional/deconvolutional layers
- Different numbers of filter sizes
- Different activation functions

Method - Architecture

U-Net with 4 convolutional-deconvolutional layers

Architecture search:

- Different numbers of convolutional/deconvolutional layers
- Different numbers of filter sizes
- Different activation functions

Modifications:

- Zero-padded convolutions for input size flexibility
- Batch normalization

Implementation

- Split of 121/5/15 for training, validation and testing

Implementation

- Split of 121/5/15 for training, validation and testing
- Patch size of 256x256

Implementation

- Split of 121/5/15 for training, validation and testing
- Patch size of 256x256
- Elimination of 'uninformative' patches
  - # foreground pixels < 10% # total pixels
  - # background pixels < 40% # total pixels

Implementation

- Split of 121/5/15 for training, validation and testing
- Patch size of 256x256
- Elimination of 'uninformative' patches
- Data augmentation: rotation, flip, elastic deformation

Implementation

- Split of 121/5/15 for training, validation and testing
- Patch size of 256x256
- Elimination of ’uninformative’ patches
- Data augmentation: rotation, flip, elastic deformation

71842 total number of patches

Method - Final Mask Generation

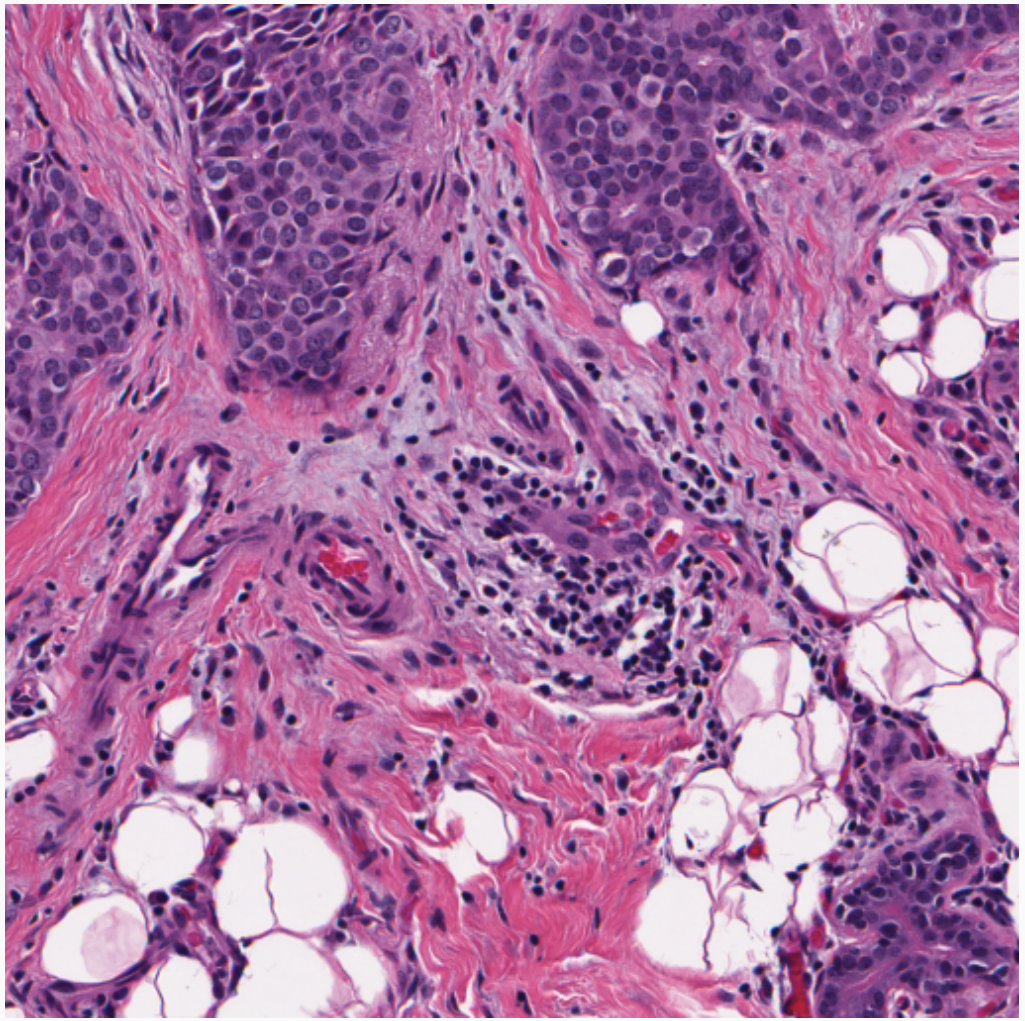

Method - Final Mask Generation

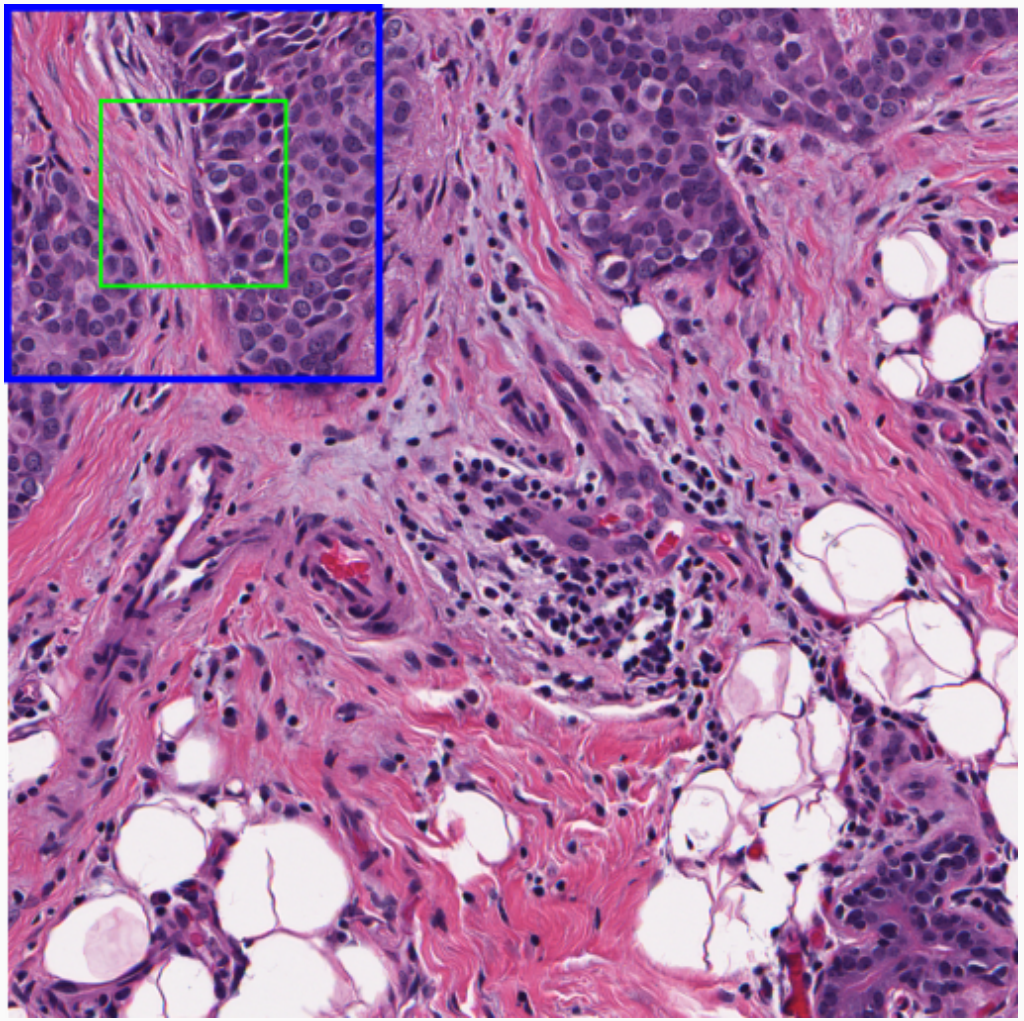

Method - Final Mask Generation

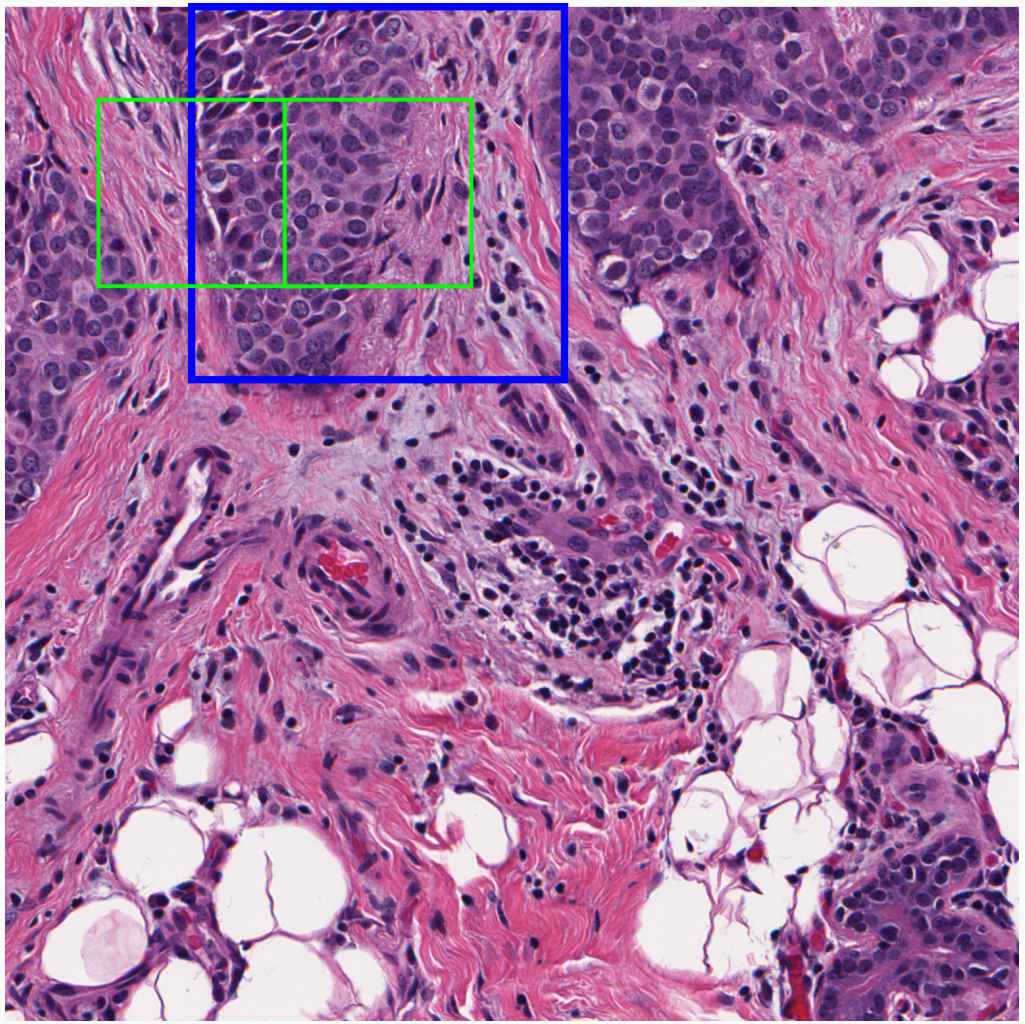

Method - Final Mask Generation

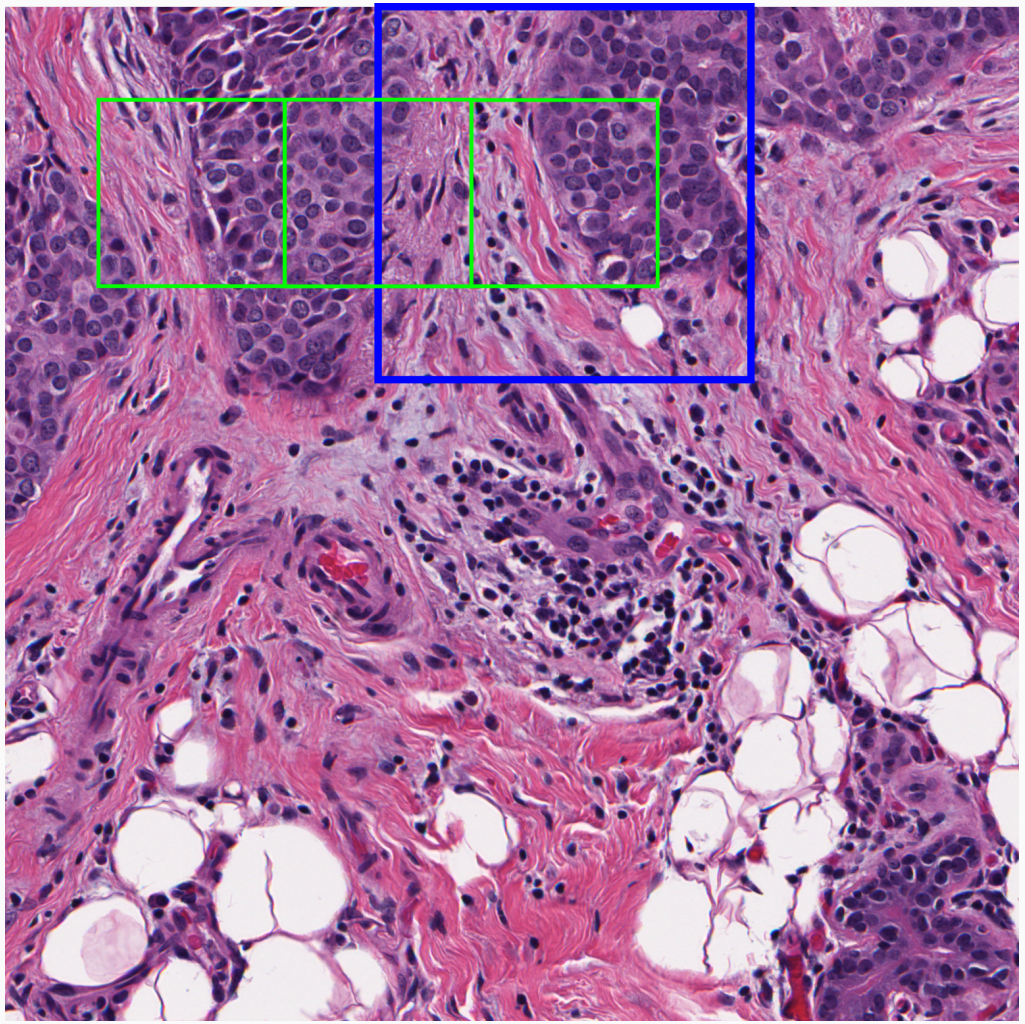

Method - Final Mask Generation

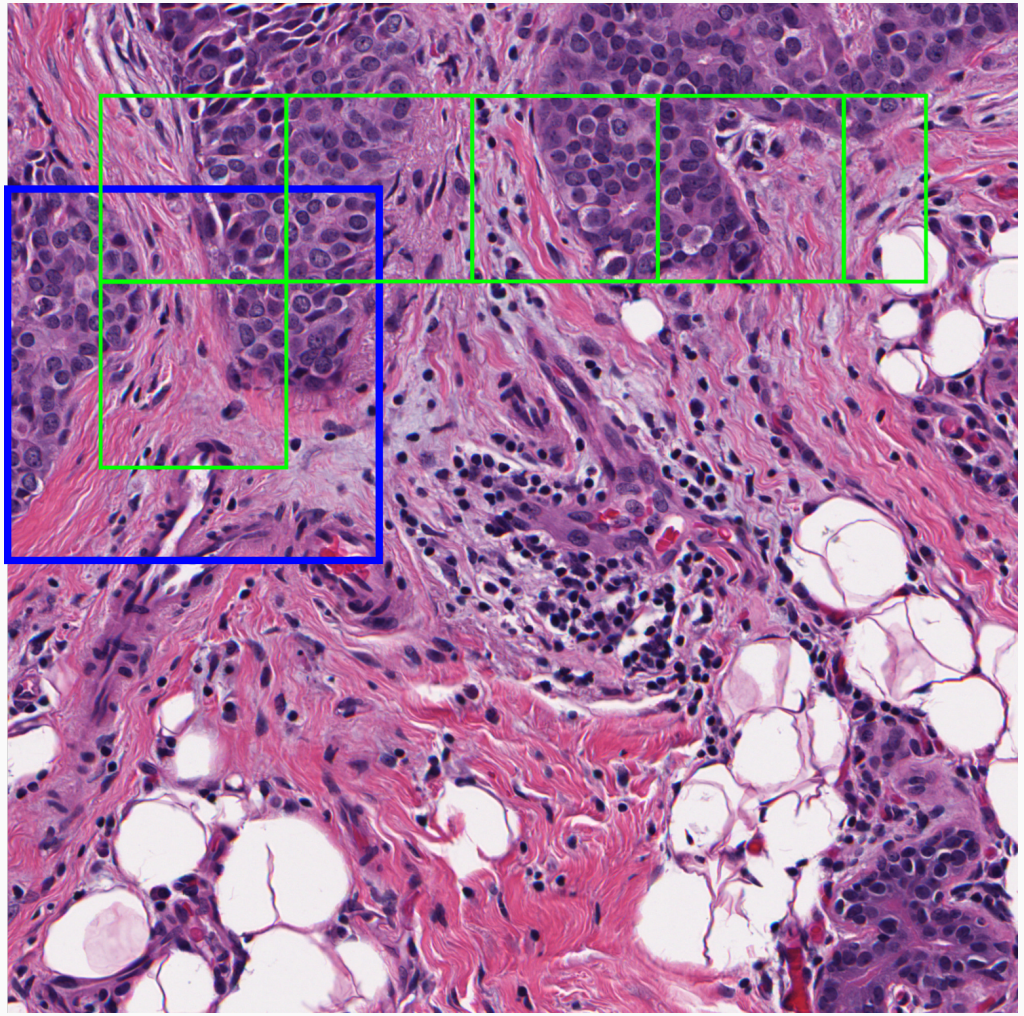

Method - Final Mask Generation

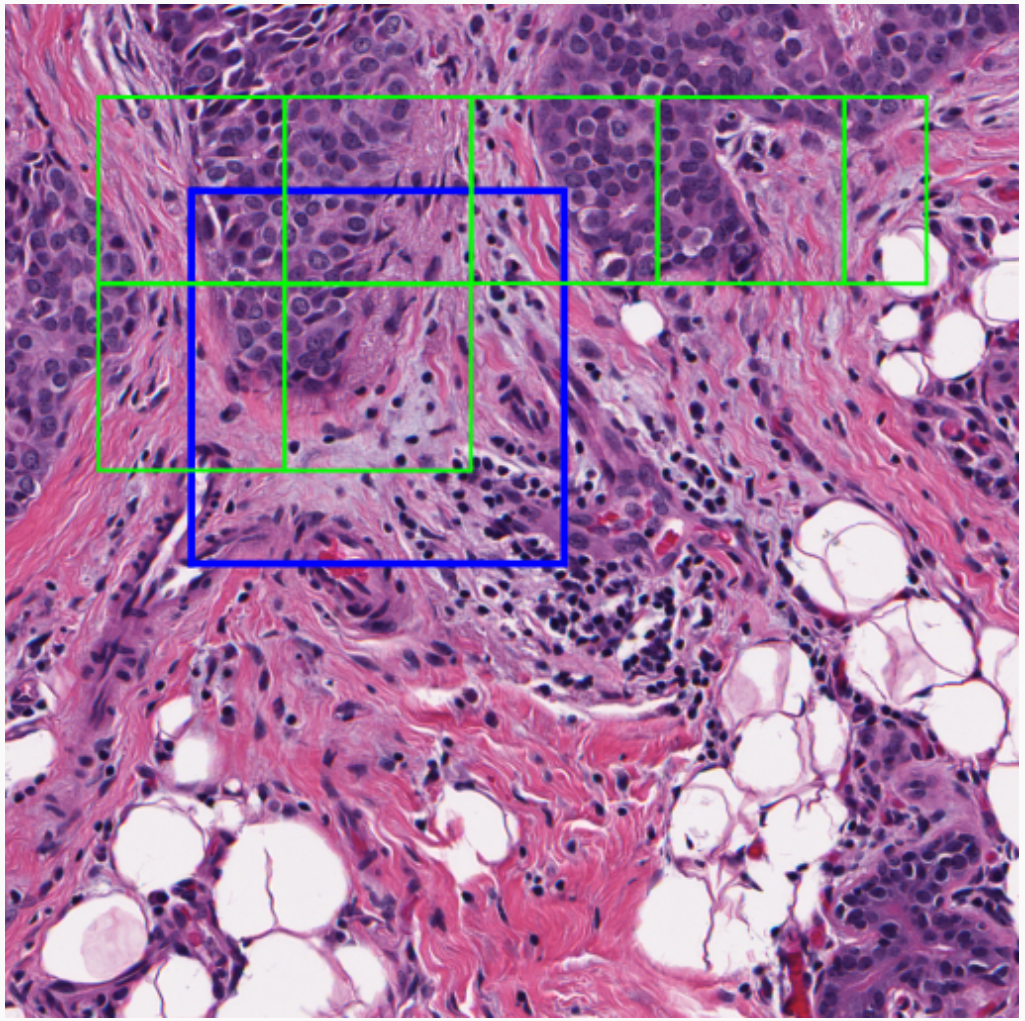

Experiments - Additional Datasets

DS1 [3]: 50 H&E images of size 500 x 500, from 11 different patients with breast cancer

- **pp**: per patient, **all**: all images/patients

[3] Naylor, P., Laé ,M., Reyal, F., and Walter, T., "Segmentation of nuclei in histopathology images by deep regression of the distance map,"IEEE Transactions on Medical Imaging, 2018

Experiments - Additional Datasets

DS1 [3]: 50 H&E images of size 500 x 500, from 11 different patients with breast cancer

- pp: per patient, all: all images/patients

DS2 [2]: 30 H&E images of size 1000 x 1000, from 7 different organs

- breast, liver, kidney, prostate, bladder, colon, stomach

[2] Kumar, N., Verma, R., Sharma, S., Bhargava, S., Vahadane, A., and Sethi, A.,"A dataset and a technique for generalized nuclear segmentation for computational pathology,"IEEE transactions on medical imaging, 2017.
[3] Naylor, P., Laé ,M., Reyal, F., and Walter, T., "Segmentation of nuclei in histopathology images by deep regression of the distance map,"IEEE Transactions on Medical Imaging, 2018

Experiments - Additional Datasets

DS1 [3]: 50 H&E images of size 500 x 500, from 11 different patients with breast cancer

- **pp**: per patient, **all**: all images/patients

DS2 [2]: 30 H&E images of size 1000 x 1000, from 7 different organs

- breast, liver, kidney, prostate, bladder, colon, stomach

! No fine tuning before testing the models on the new datasets

[2] Kumar, N., Verma, R., Sharma, S., Bhargava, S., Vahadane, A., and Sethi, A.,"A dataset and a technique for generalized nuclear segmentation for computational pathology,"IEEE transactions on medical imaging, 2017.
[3] Naylor, P., Laé ,M., Reyal, F., and Walter, T., "Segmentation of nuclei in histopathology images by deep regression of the distance map,"IEEE Transactions on Medical Imaging, 2018

Experiments - Evaluation Metrics

Pixel-based Evaluation Metrics:

recall, precision, F1-score, accuracy, Jaccard Index

Experiments - Evaluation Metrics

Pixel-based Evaluation Metrics:

recall, precision, F1-score, accuracy, Jaccard Index

Object-based Evaluation Metrics:

$G = \bigcup_{i=1}^{K} G_i$ GT nuclei pixels, $P = \bigcup_{j=1}^{L} P_j$ predicted nuclei pixels

Experiments - Evaluation Metrics

Pixel-based Evaluation Metrics:

recall, precision, F1-score, accuracy, Jaccard Index

Object-based Evaluation Metrics:

$G = \bigcup_{i=1}^{K} G_i$ GT nuclei pixels, $P = \bigcup_{j=1}^{L} P_j$ predicted nuclei pixels

$$\text{Jaccard Index (JI)} = \frac{G \cap P}{G \cup P}$$

Experiments - Evaluation Metrics

Pixel-based Evaluation Metrics:

recall, precision, F1-score, accuracy, Jaccard Index

Object-based Evaluation Metrics:

$G = \bigcup_{i=1}^{K} G_i$ GT nuclei pixels, $P = \bigcup_{j=1}^{L} P_j$ predicted nuclei pixels

$$\text{Jaccard Index (JI)} = \frac{G \cap P}{G \cup P}$$

$$\text{Aggregated Jaccard Index (AJI)} = \frac{\sum_{i=1}^{L} |G_i \cap P_j^*(i)|}{\sum_{i=1}^{K} |G_i \cup P_j^*(i)| + \sum_{k \in U} |P_k|}$$

where $P_j^*(i) \leftarrow \arg\max \frac{G_i \cap P_j}{G_i \cup P_j} \quad \forall i$

U: set of all unassigned nuclei

Experiments - Evaluation Metrics

Pixel-based Evaluation Metrics:

recall, precision, F1-score, accuracy, Jaccard Index

Object-based Evaluation Metrics:

$G = \bigcup_{i=1}^{K} G_i$ GT nuclei pixels, $P = \bigcup_{j=1}^{L} P_j$ predicted nuclei pixels

$$\text{Jaccard Index (JI)} = \frac{G \cap P}{G \cup P}$$

$$\text{Aggregated Jaccard Index (AJI)} = \frac{\sum_{i=1}^{L} |G_i \cap P_j^*(i)|}{\sum_{i=1}^{K} |G_i \cup P_j^*(i)| + \sum_{k \in U} |P_k|}$$

$$\text{where} \quad P_j^*(i) \leftarrow \arg\max \frac{G_i \cap P_j}{G_i \cup P_j} \quad \forall i$$

U: set of all unassigned nuclei

Experiments - Evaluation Metrics

Pixel-based Evaluation Metrics:

recall, precision, F1-score, accuracy, Jaccard Index

Object-based Evaluation Metrics:

$G = \bigcup_{i=1}^{K} G_i$ GT nuclei pixels, $P = \bigcup_{j=1}^{L} P_j$ predicted nuclei pixels

$$\text{Jaccard Index (JI)} = \frac{G \cap P}{G \cup P}$$

$$\text{Aggregated Jaccard Index (AJI)} = \frac{\sum_{i=1}^{L} |G_i \cap P_j^*(i)|}{\sum_{i=1}^{K} |G_i \cup P_j^*(i)| + \sum_{k \in U} |P_k|}$$

where $P_j^*(i) \leftarrow \arg\max \frac{G_i \cap P_j}{G_i \cup P_j} \quad \forall i$

U: set of all unassigned nuclei

Experiments - Quantitative Analysis

			Recall	Precision	F1 score	Accuracy	JI (IoU)	AJI	Time (sec)
DS 1	pp	[1]	0.35 (0.21)	**0.91 (0.06)**	0.45 (0.21)	0.92 (0.02)	0.32 (0.18)	0.84 (0.04)	467.88 (13.67)
		Proposed	**0.60 (0.14)**	0.89 (0.04)	**0.70 (0.10)**	**0.94 (0.02)**	**0.55 (0.11)**	**0.88 (0.03)**	**0.47 (0.01)**
	all	[1]	0.33 (0.23)	**0.92 (0.08)**	0.44 (0.23)	0.92 (0.06)	0.31 (0.20)	0.85 (0.10)	467.88 (13.67)
		Proposed	**0.60 (0.17)**	0.90 (0.06)	**0.70 (0.13)**	**0.94 (0.04)**	**0.55 (0.14)**	**0.89 (0.08)**	**0.47 (0.01)**
DS 2		[1]	0.59 (0.23)	0.81 (0.15)	0.63 (0.18)	0.85 (0.08)	0.49 (0.17)	0.70 (0.14)	1642.99 (39.91)
		Proposed	**0.73 (0.16)**	**0.82 (0.09)**	**0.76 (0.12)**	**0.89 (0.06)**	**0.62 (0.13)**	**0.78 (0.10)**	**1.84 (0.06)**

[1] Janowczyk, A., and Madabhushi, A., “Deep learning for digital pathology image analysis: A comprehensive tutorial with selected use cases,” Journal of pathology informatics, 2016.

Experiments - Quantitative Analysis

			Recall	Precision	F1 score	Accuracy	JI (IoU)	AJI	Time (sec)
DS 1	pp	[1]	0.35 (0.21)	**0.91 (0.06)**	0.45 (0.21)	0.92 (0.02)	0.32 (0.18)	0.84 (0.04)	467.88 (13.67)
		Proposed	**0.60 (0.14)**	0.89 (0.04)	**0.70 (0.10)**	**0.94 (0.02)**	**0.55 (0.11)**	**0.88 (0.03)**	**0.47 (0.01)**
	all	[1]	0.33 (0.23)	**0.92 (0.08)**	0.44 (0.23)	0.92 (0.06)	0.31 (0.20)	0.85 (0.10)	467.88 (13.67)
		Proposed	**0.60 (0.17)**	0.90 (0.06)	**0.70 (0.13)**	**0.94 (0.04)**	**0.55 (0.14)**	**0.89 (0.08)**	**0.47 (0.01)**
DS 2		[1]	0.59 (0.23)	0.81 (0.15)	0.63 (0.18)	0.85 (0.08)	0.49 (0.17)	0.70 (0.14)	1642.99 (39.91)
		Proposed	**0.73 (0.16)**	**0.82 (0.09)**	**0.76 (0.12)**	**0.89 (0.06)**	**0.62 (0.13)**	**0.78 (0.10)**	**1.84 (0.06)**

[1] Janowczyk, A., and Madabhushi, A., "Deep learning for digital pathology image analysis: A comprehensive tutorial with selected use cases," Journal of pathology informatics, 2016.

Experiments - Quantitative Analysis

			Recall	Precision	F1 score	Accuracy	JI (IoU)	AJI	Time (sec)
DS 1	pp	[1]	0.35 (0.21)	**0.91 (0.06)**	0.45 (0.21)	0.92 (0.02)	0.32 (0.18)	0.84 (0.04)	467.88 (13.67)
		Proposed	**0.60 (0.14)**	0.89 (0.04)	**0.70 (0.10)**	**0.94 (0.02)**	**0.55 (0.11)**	**0.88 (0.03)**	**0.47 (0.01)**
	all	[1]	0.33 (0.23)	**0.92 (0.08)**	0.44 (0.23)	0.92 (0.06)	0.31 (0.20)	0.85 (0.10)	467.88 (13.67)
		Proposed	**0.60 (0.17)**	0.90 (0.06)	**0.70 (0.13)**	**0.94 (0.04)**	**0.55 (0.14)**	**0.89 (0.08)**	**0.47 (0.01)**
DS 2		[1]	0.59 (0.23)	0.81 (0.15)	0.63 (0.18)	0.85 (0.08)	0.49 (0.17)	0.70 (0.14)	1642.99 (39.91)
		Proposed	**0.73 (0.16)**	**0.82 (0.09)**	**0.76 (0.12)**	**0.89 (0.06)**	**0.62 (0.13)**	**0.78 (0.10)**	**1.84 (0.06)**

[3] on DS1 (trained with DS2): 0.81 mean F1, 0.56 mean AJI

[3] on DS1 (trained with DS1 & DS2): 0.81 mean F1, 0.57 mean AJI

[1] Janowczyk, A., and Madabhushi, A., "Deep learning for digital pathology image analysis: A comprehensive tutorial with selected use cases," Journal of pathology informatics, 2016.
[2] Kumar, N., Verma, R., Sharma, S., Bhargava, S., Vahadane, A., and Sethi, A.,"A dataset and a technique for generalized nuclear segmentation for computational pathology,"IEEE transactions on medical imaging, 2017.
[3] Naylor, P., Laé ,M., Reyal, F., and Walter, T., "Segmentation of nuclei in histopathology images by deep regression of the distance map,"IEEE Transactions on Medical Imaging, 2018

Experiments - Quantitative Analysis

			Recall	Precision	F1 score	Accuracy	JI (IoU)	AJI	Time (sec)
DS 1	pp	[1]	0.35 (0.21)	**0.91 (0.06)**	0.45 (0.21)	0.92 (0.02)	0.32 (0.18)	0.84 (0.04)	467.88 (13.67)
		Proposed	**0.60 (0.14)**	0.89 (0.04)	**0.70 (0.10)**	**0.94 (0.02)**	**0.55 (0.11)**	**0.88 (0.03)**	**0.47 (0.01)**
	all	[1]	0.33 (0.23)	**0.92 (0.08)**	0.44 (0.23)	0.92 (0.06)	0.31 (0.20)	0.85 (0.10)	467.88 (13.67)
		Proposed	**0.60 (0.17)**	0.90 (0.06)	**0.70 (0.13)**	**0.94 (0.04)**	**0.55 (0.14)**	**0.89 (0.08)**	**0.47 (0.01)**
DS 2		[1]	0.59 (0.23)	0.81 (0.15)	0.63 (0.18)	0.85 (0.08)	0.49 (0.17)	0.70 (0.14)	1642.99 (39.91)
		Proposed	**0.73 (0.16)**	**0.82 (0.09)**	**0.76 (0.12)**	**0.89 (0.06)**	**0.62 (0.13)**	**0.78 (0.10)**	**1.84 (0.06)**

[3] on DS1 (trained with DS2): 0.81 mean F1, 0.56 mean AJI

[3] on DS1 (trained with DS1 & DS2): 0.81 mean F1, 0.57 mean AJI

MoNuSeg Challenge @ MICCAI 2018 (trained with DS2):

Top three performing algorithms: 0.6907, 0.6868, 0.6852 mean AJI

[1] Janowczyk, A., and Madabhushi, A., "Deep learning for digital pathology image analysis: A comprehensive tutorial with selected use cases," Journal of pathology informatics, 2016.
[2] Kumar, N., Verma, R., Sharma, S., Bhargava, S., Vahadane, A., and Sethi, A.,"A dataset and a technique for generalized nuclear segmentation for computational pathology,"IEEE transactions on medical imaging, 2017.
[3] Naylor, P., Laé ,M., Reyal, F., and Walter, T., "Segmentation of nuclei in histopathology images by deep regression of the distance map,"IEEE Transactions on Medical Imaging, 2018

Experiments - Qualitative Analysis

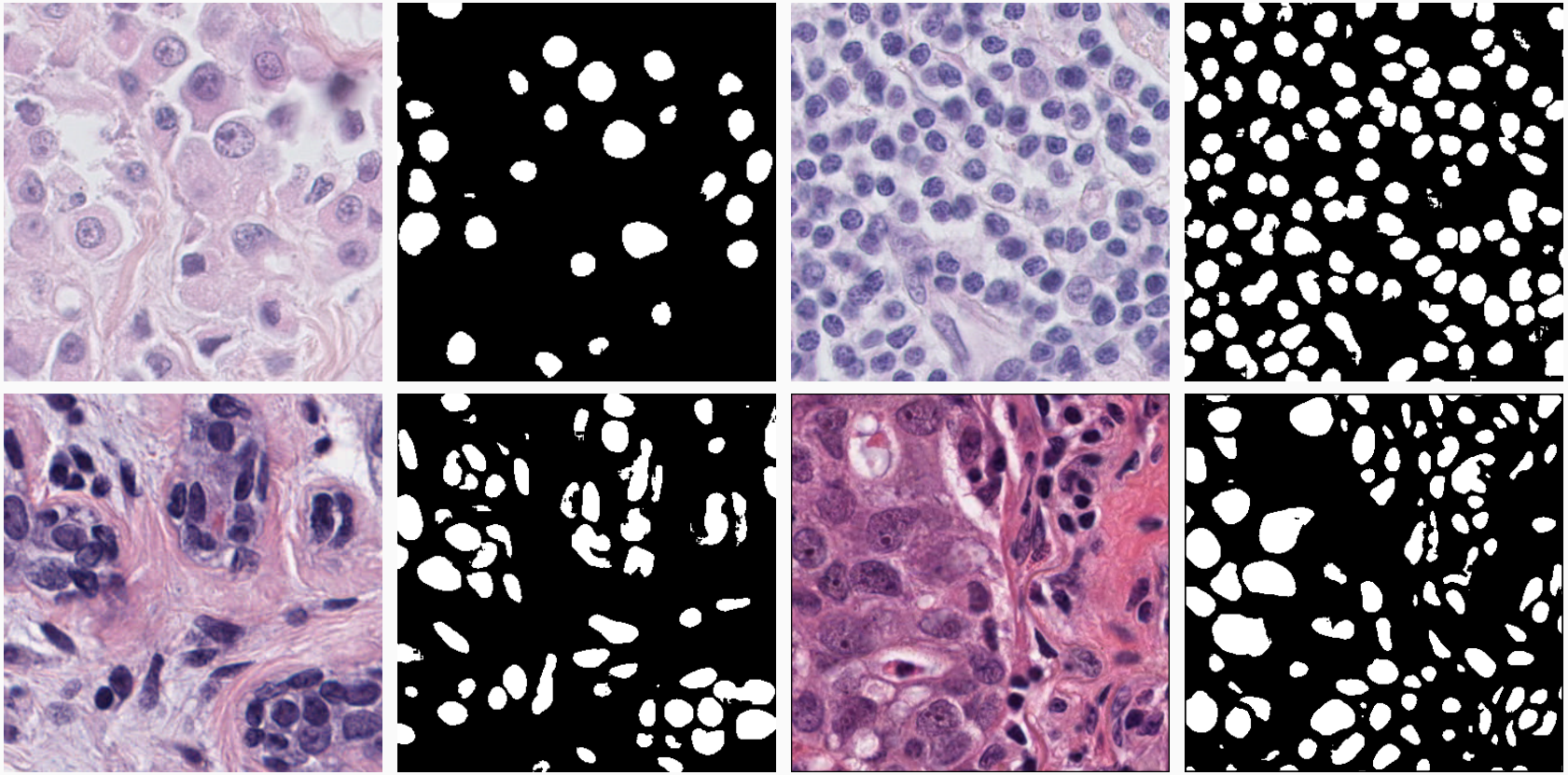

Conclusion

Conclusion

- We proposed a method for nuclei segmentation in histapathology images using incomplete ground truth information

Conclusion

- We proposed a method for nuclei segmentation in histapathology images using incomplete ground truth information
- Incorporation of prior knowledge, even with uncertainty, helps us to design more efficient models/algorithms

Conclusion

- We proposed a method for nuclei segmentation in histapathology images using incomplete ground truth information
- Incorporation of prior knowledge, even with uncertainty, helps us to design more efficient models/algorithms
- Pixel-based processing for holistic tasks is not efficient

Conclusion

- We proposed a method for nuclei segmentation in histapathology images using incomplete ground truth information
- Incorporation of prior knowledge, even with uncertainty, helps us to design more efficient models/algorithms
- Pixel-based processing for holistic tasks is not efficient
- There exists an open-source plug&play model for nuclei segmentation: at least a point you can start with

Questions?

Deniz Mercadier Sayın*, Beril Besbinar†, Pascal Frossard†
beril.besbinar@epfl.ch
†EPFL - Signal Processing Laboratory (LTS4)

Evaluation Metrics

Pixel-based Evaluation Metrics:

TN: True Negative
TP: True Positive
FN: False Negative
FP: False Positive

		Predicted: Negative	Predicted: Positive
Actual	Negative	TN	FP
	Positive	FN	TP

$$\text{recall} = \frac{TP}{TP + FN} \qquad \text{F1 score} = 2 * \frac{\text{precision} * \text{recall}}{\text{precision} + \text{recall}}$$

$$\text{precision} = \frac{TP}{TP + FP} \qquad \text{accuracy} = \frac{TP + TN}{TP + TN + FP + FN}$$

$$\text{Jaccard Index (JI)} = \frac{TP}{TP + FN + FP}$$

Final Mask Generation

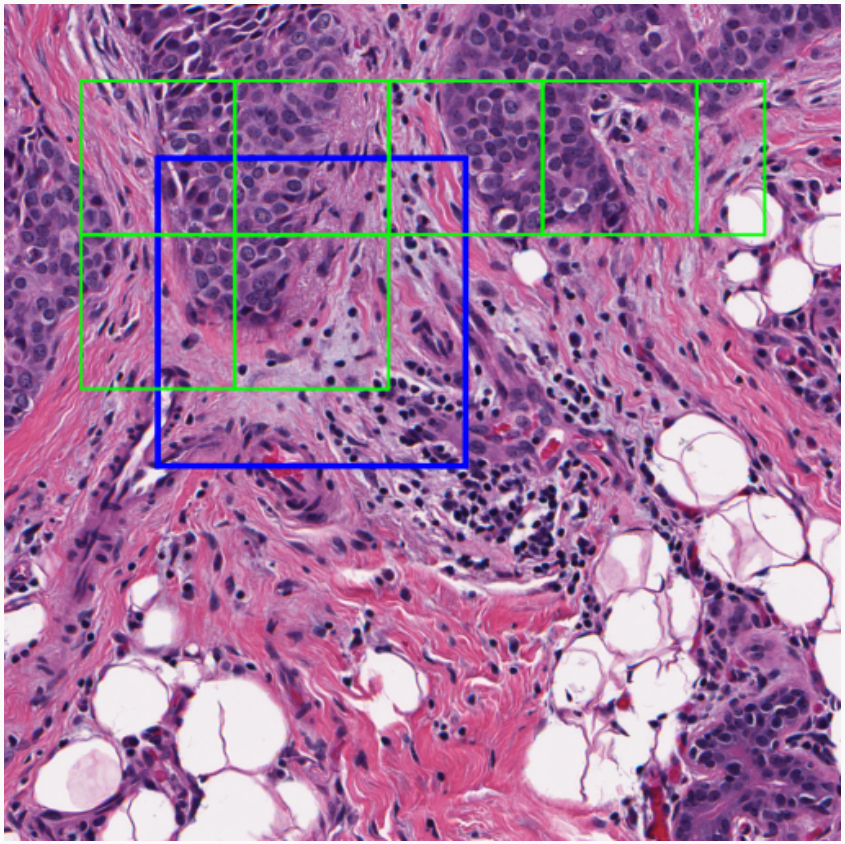

For an 2000x2000 image

- patches of size 256x256: 256 patches
- pixel-based processing by patches of size 32x32: ≈ 3.88m patches

Quantitative Analysis

			Recall	Precision	F1 score	Accuracy	JI (IoU)	AJI	Time (sec)
DS 1	pp	[1]	0.35 (0.21)	**0.91 (0.06)**	0.45 (0.21)	0.92 (0.02)	0.32 (0.18)	0.84 (0.04)	467.88 (13.67)
		Proposed	**0.60 (0.14)**	0.89 (0.04)	**0.70 (0.10)**	**0.94 (0.02)**	**0.55 (0.11)**	**0.88 (0.03)**	**0.47 (0.01)**
	all	[1]	0.33 (0.23)	**0.92 (0.08)**	0.44 (0.23)	0.92 (0.06)	0.31 (0.20)	0.85 (0.10)	467.88 (13.67)
		Proposed	**0.60 (0.17)**	0.90 (0.06)	**0.70 (0.13)**	**0.94 (0.04)**	**0.55 (0.14)**	**0.89 (0.08)**	**0.47 (0.01)**
DS 2		[1]	0.59 (0.23)	0.81 (0.15)	0.63 (0.18)	0.85 (0.08)	0.49 (0.17)	0.70 (0.14)	1642.99 (39.91)
		Proposed	**0.73 (0.16)**	**0.82 (0.09)**	**0.76 (0.12)**	**0.89 (0.06)**	**0.62 (0.13)**	**0.78 (0.10)**	**1.84 (0.06)**

		F1	AJI
DS 1	[2]	0.72	0.54
	[3] trained with DS2	0.81	0.56
	[3] trained with DS1 & DS2	0.81	0.57
	[3] trained only on Breast	0.82	0.59

MoNuSeg Challenge @ MICCAI 2018 (trained with DS2):

Top three performing algorithms: 0.6907, 0.6868, 0.6852 mean AJI

[1] Janowczyk, A., and Madabhushi, A., “Deep learning for digital pathology image analysis: A comprehensive tutorial with selected use cases,” Journal of pathology informatics, 2016.

[2] Kumar, N., Verma, R., Sharma, S., Bhargava, S., Vahadane, A., and Sethi, A.,“A dataset and a technique for generalized nuclear segmentation for computational pathology,”IEEE transactions on medical imaging, 2017.

[3] Naylor, P., Laé ,M., Reyal, F., and Walter, T., “Segmentation of nuclei in histopathology images by deep regression of the distance map,”IEEE Transactions on Medical Imaging, 2018

Experiments - Qualitative Analysis

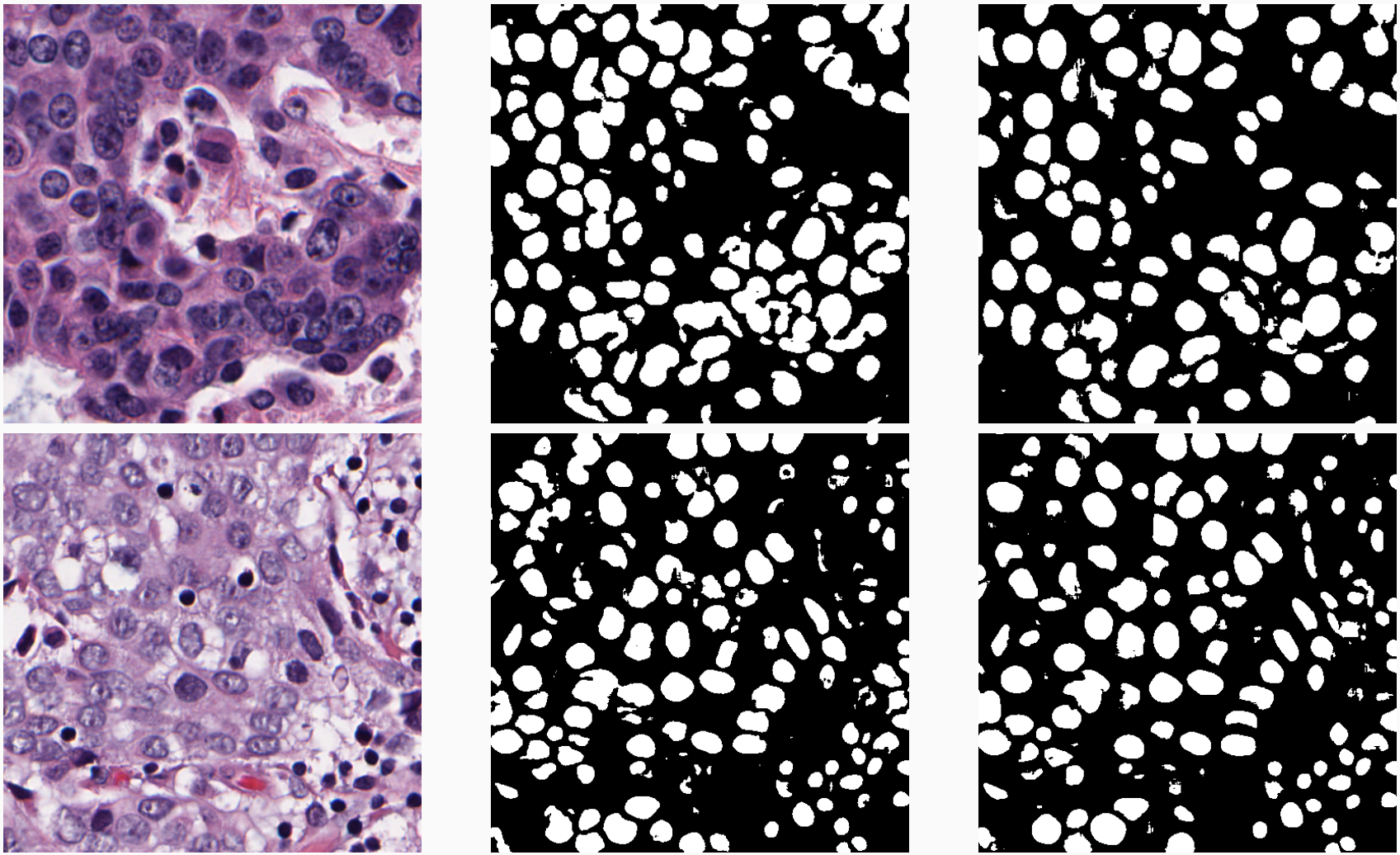

Image | Janowczyk et al. | Proposed method